Atherosclerosis 223 (2012) 321–326

Contents lists available at SciVerse ScienceDirect

Atherosclerosis

journal homepage: www.elsevier.com/locate/atherosclerosis

Critical mechanical conditions around neovessels in carotid atherosclerotic plaque may promote intraplaque hemorrhage

Zhongzhao Teng [a,b,*], Jing He [a], Andrew J. Degnan [c], Shengyong Chen [d], Umar Sadat [e], Nasim Sheikh Bahaei [a], James H.F. Rudd [f], Jonathan H. Gillard [a]

[a] University Department of Radiology, University of Cambridge, UK
[b] Department of Engineering, University of Cambridge, UK
[c] School of Medicine, The George Washington University, USA
[d] College of Computer Science and Technology, Zhejiang University of Technology, Hangzhou, China
[e] Department of Surgery, Cambridge University Hospitals NHS Foundation Trust, Cambridge, UK
[f] Division of Cardiovascular Medicine, University of Cambridge, UK

ARTICLE INFO

Article history:
Received 5 April 2012
Received in revised form
1 June 2012
Accepted 11 June 2012
Available online 21 June 2012

Keywords:
Carotid atherosclerosis
Intraplaque hemorrhage
Neovascularization
Mechanics
Deformation

ABSTRACT

Objective: Intraplaque hemorrhage is an increasingly recognized contributor to plaque instability. Neovascularization of plaque is believed to facilitate the entry of inflammatory and red blood cells (RBC). Under physiological conditions, neovessels are subject to mechanical loading from the deformation of atherosclerotic plaque by blood pressure and flow. Local mechanical environments around neovessels and their relevant pathophysiologic significance have not yet been examined.

Methods and results: Four carotid plaque samples removed at endarterectomy were collected for histopathological examination. Neovessels and other components were manually segmented to build numerical models for mechanical analysis. Each component was assumed to be non-linear isotropic, piecewise homogeneous and incompressible. The results indicated that local maximum principal stress and stretch and their variations during one cardiac cycle were greatest around neovessels. Neovessels surrounded by RBC underwent a much larger stretch during systole than those without RBCs present nearby (median [inter quartile range]; 1.089 [1.056, 1.131] vs. 1.034 [1.020, 1.067]; $p < 0.0001$) and much larger stress (5.3 kPa [3.4, 8.3] vs. 3.1 kPa [1.6, 5.5]; $p < 0.0001$) and stretch (0.0282 [0.0190, 0.0427] vs. 0.0087 [0.0045, 0.0185]; $p < 0.0001$) variations during the cardiac cycle.

Conclusions: Local critical mechanical conditions may lead to the rupture of neovessels resulting in the formation and expansion of intraplaque hemorrhage.

1. Introduction

Stroke is the third leading cause of death and the primary cause of disability in the world [1]. Carotid atherosclerotic disease is thought to be the predominant etiology of stroke in Western society [2]. Nevertheless, clinical assessment of stroke risk has not progressed beyond the use of luminal stenosis in spite of evidence to suggest that this is an inadequate predictor of stroke [3]. Recent imaging studies have suggested plaque composition as an independent risk factor for ischemic stroke [4,5].

A typical carotid atherosclerotic plaque is composed of lipid-rich necrotic core (LRNC), calcium and plaque hemorrhage covered by a layer of fibrous cap (FC). High risk characteristics include large LRNC [6], presence of hemorrhage [7], and thin or defective FC [8]. Intraplaque hemorrhage (IPH) may cause complications by promoting vulnerability, luminal occlusion or downstream emboli. Long term plaque progression due to IPH can be captured using high-resolution magnetic resonance imaging (MRI) [9]. It has been observed that IPH has a much wider prevalence in symptomatic patients than asymptomatic individuals [5]. Altaf et al. found that 15 out of 66 recurrent events were associated with IPH while only two recurrent events occurred in its absence in symptomatic patients with high-grade atherosclerotic lesions [10]. Similar results were obtained from 39 symptomatic patients with mild to moderate (30–69%) stenosis [11]. Recently, in a prospective study of 61 acutely symptomatic patients, Sadat et al. found that the

* Corresponding author. Department of Engineering, Level 5, Box 218, University of Cambridge, Addenbrooke's Hospital Hills Road, Cambridge CB2 0QQ, UK. Tel.: +44 01223 746447; fax: +44 01223 330915.
E-mail address: zt215@cam.ac.uk (Z. Teng).

0021-9150/$ – see front matter © 2012 Elsevier Ireland Ltd. All rights reserved.
http://dx.doi.org/10.1016/j.atherosclerosis.2012.06.015

presence of plaque hemorrhage was closely associated with the occurrence of future cerebrovascular events [12]. Even in asymptomatic patients, there is a risk conferred by IPH. Takaya et al. found that presence of IPH was associated with the incidence of cerebrovascular events in previously asymptomatic patients ($n = 154$; stenosis: 50–79%) [13]. Singh et al. confirmed that MR-depicted IPH was associated with an increased risk of cerebrovascular events ($n = 91$) in asymptomatic moderate carotid stenosis [14].

Histopathological examinations have revealed the association between IPH and the presence of neovessels [15,16]. Neovascularization can be considered a compensatory response to hypoxia present in the deep intimal and medial areas of the artery [17,18]. Due to poorly developed vessel walls, blood components, such as red blood cells (RBC), neutrophils and other proinflammatory cells, may migrate from the bloodstream into the plaque [19,20]. These may release an array of proteases that induce the death of endothelial cells, thereby generating local disruption of microvessels [21] and further promoting IPH.

Aside from these inflammatory factors, under physiological conditions, atherosclerotic plaque is subjected to mechanical loading due to blood pressure, as are its associated neovessels. Finite element analysis has been widely used to estimate the stress concentrated within the fibrous cap as a mechanics-based vulnerability assessment [22,23]. This is based on the hypothesis that fibrous cap rupture possibly occurs when the extra loading due to blood pressure and hemodynamic flow exceed its material strength. Being embedded in the atherosclerotic plaque, neovessels are also presumably susceptible to mechanical loading effects from the deformation of entire plaque structure driven by the dynamic blood pressure. Harsh local mechanical conditions, if present, may also contribute to the neovessel damage and further encourage IPH formation. However, this has not yet been examined in detail. This study, therefore, aims to (1) quantify the critical mechanical conditions (stress and stretch) around neovessels based on high-resolution histological images; and (2) characterize the association between these conditions and plaque's pathological features, such as the distribution of red blood cells as a marker of IPH.

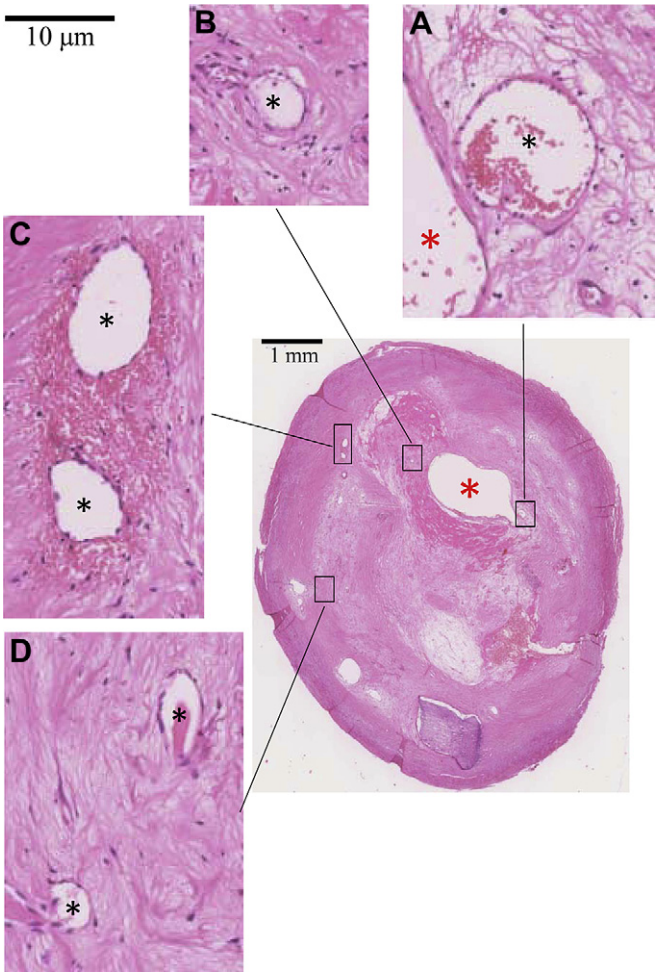

Fig. 1. Microscopic slide (H&E) showing plaque structures (A&B: neovessels closed to the main arterial lumen; C: neovessels located in the middle region with abundant adjacent red blood cells; and D: neovessels located in a peripheral region; red asterisk stands for the main arterial lumen and black asterisk for the lumen of neovessel).

2. Materials and methods

Four carotid plaques with over 70% stenosis were collected *en bloc* following carotid endarterectomy. One of the four patients was male; they were 74.3 ± 15.2 years old; the blood pressure was 127.5 ± 26.8 mmHg for systole and 78.0 ± 15.0 mmHg for diastole. The samples were formalin-saline fixed, decalcified, embedded in paraffin and stained using hematoxylin and eosin (H&E), Verhoeff's Van Gieson (EVG), Nile red and Masson's trichrome to visualize various components within plaque. Histopathological slides were digitalized using NanoZoomer (Hamamatsu, Japan) (Fig. 1). Considering the computational workload, one slide located at the most stenotic site was chosen for analysis.

The digitalized image was segmented manually using NDP Viewer (Hamamatsu, Japan) to identify the lumen contour, fibrous tissue, lipid and hemorrhage, etc. The contours of lumen and outer wall of each neovessel were carefully traced at 40× magnification. About 100 neovessels were identified for each slide. All contours were exported and processed using an in-house developed package in Matlab (MathWorks, USA). All components were assumed to be non-linear hyper-elastic, piecewise homogeneous and incompressible materials governed by the modified Mooney–Rivlin strain energy density function,

$$W = c_1(I_1 - 3) + D_1 \exp[D_2(I_1 - 3) - 1]$$

where I_1 is the first strain invariant and c_1, D_1 and D_2 are material parameters, derived from earlier studies [24] with the following details: vessel material: $c_1 = 36.8$ kPa, $D_1 = 14.4$ kPa, $D_2 = 2$; fibrous cap: $c_1 = 73.6$ kPa, $D_1 = 28.8$ kPa, $D_2 = 2.5$; lipid core: $c_1 = 2$ kPa, $D_1 = 2$ kPa, $D_2 = 1.5$: calcification, $c_1 = 368$ kPa, $D_1 = 144$ kPa, $D_2 = 2.0$; fresh IPH: $c_1 = 1$ kPa, $D_1 = 1$ kPa, $D_2 = 0.25$ and for chronic IPH: $c_1 = 9$ kPa, $D_1 = 9$ kPa, $D_2 = 0.25$. The blood pressure of each patient was used as the loading condition applying on the plaque as a whole and the pressure in the neovessel was assumed to be 10 mmHg (as it was not directly measurable). This value was chosen because it approximately reflects blood pressure in the venous environment. However, our experimental conclusions did not change when the value was lowered to 5 mmHg. Considering the small size of an individual neovessel, a very fine mesh was used around the local region with about 0.5 μm on each element edge. Each model consists of over 100,000 elements. Maximum principal stress (Stress-P_1) and stretch (Stretch-P_1) were computed using finite element method (FEM) in ADINA8.6.1 (ADINA R&D, Inc., USA).

The region of interest (ROI) for each neovessel was defined as the region within four times of the corresponding lumen area (The number could be changed to 2.5, 6 and 8 and the results and conclusions remained the same). The maximum value of Stress-P_1 and Stretch-P_1 within ROI was extracted from the simulation. The value at systole and the difference across the cardiac cycle were used to quantify the critical mechanical condition. The change of

lumen area of the neovessel during the cardiac cycle was also computed to quantify the deformation. The locations of red blood cells were recorded to quantify their distribution. Therefore, the neovessels were divided into two groups (without-RBC and with-RBC) depending on the presence of red blood cell within the ROI. The association between this distribution and critical mechanical condition was further analyzed.

The statistical analysis was performed in Instat3.06 (GraphPad Software Inc., USA). A two-tailed Mann–Whitney test was used for the statistical analysis if the data did not pass the normality test (Shapiro–Wilk test); otherwise, two-tailed student *t* test was used. A significant difference was assumed with a p-value <0.05.

3. Results

In total, 379 neovessels were identified in four histological slides. Red blood cells were found within the region of interest of 146 of them (38.5%). As it can be seen from Fig. 1, neovessels appeared throughout the plaque structure and many were adjacent to the lumen (Fig. 1A&B), some were located in the middle of the plaque (Fig. 1C) surrounded by a cluster of red blood cells and some were located in the periphery of the plaque (Fig. 1D) with various lumen sizes and wall thicknesses. The corresponding band plot of Stretch-P_1 was shown in Fig. 2. As depicted in the amplified thumbnails, large deformations were found around the neovessel when it was close to the lumen (Fig. 2A, B & C). Fig.3 visualizes the location-dependent mechanical parameters, stress concentration at systole (Stress-P_1; Fig.3A), stress variation during one cardiac cycle (Diff-Stress-P_1; Fig.3B), large local deformation at systole (Stretch-P_1; Fig.3C) and the stretch variation (Diff-Stretch-P_1; Fig.3D), in the ROI of each neovessel. These parameters decrease greatly when the neovessel is located away from the carotid lumen.

The harsh mechanical environment around neovessels may be associated with the leak of red blood cells, which were found

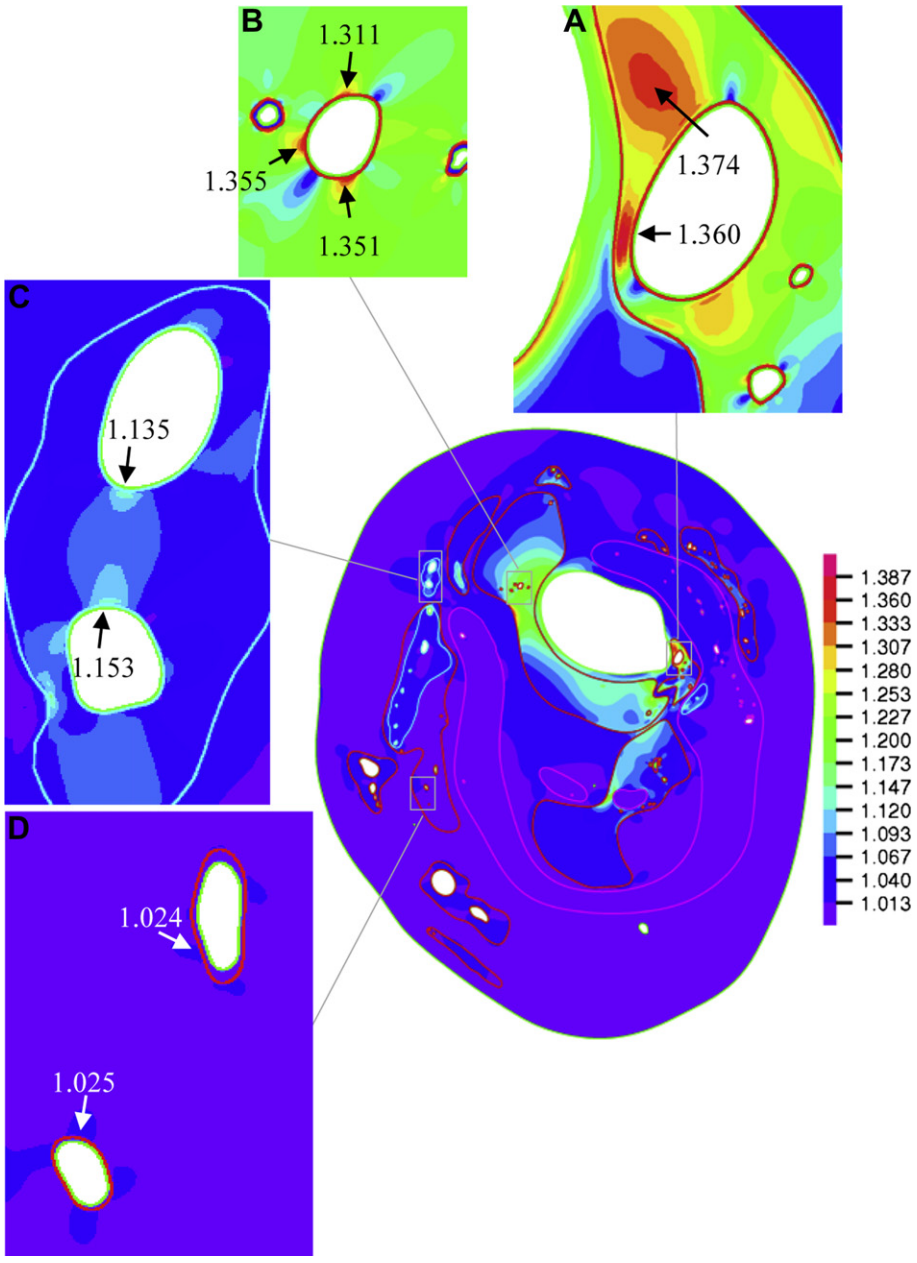

Fig. 2. The band plot of maximum principal stretch (Stretch-P_1) at systole (the insets showing the local deformation around the corresponding neovessel amplified in Fig. 1).

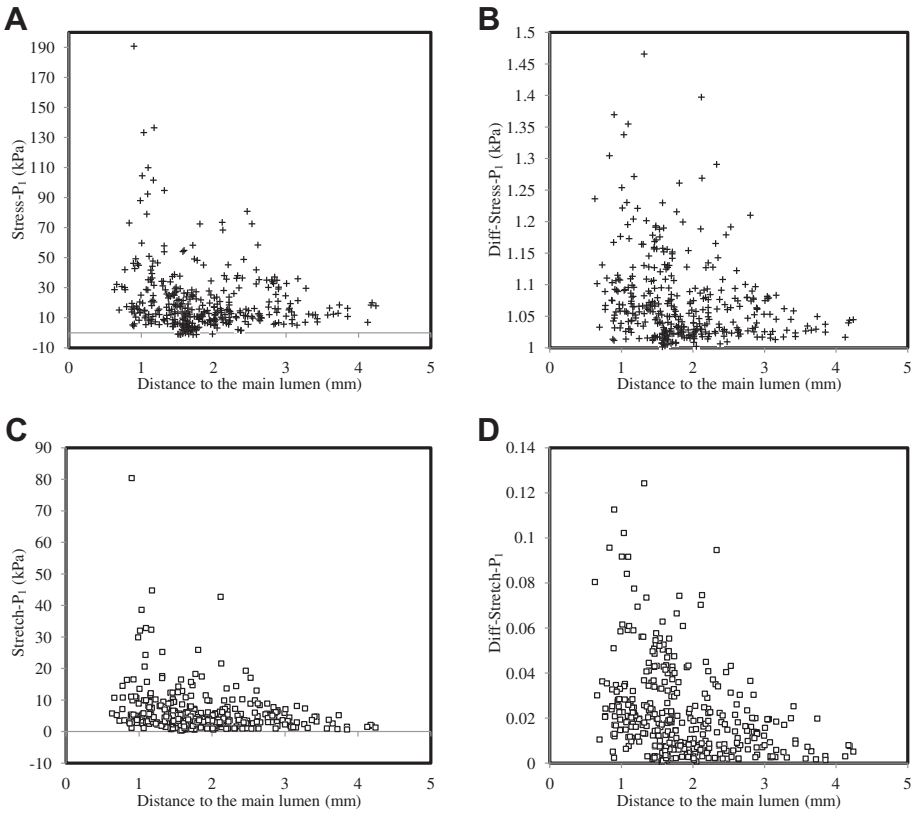

Fig. 3. The relationship between critical mechanical conditions around the neovessel and its distance from the main arterial lumen (A: Stress-P_1; B: variation of Stress-P_1 during one cardiac cycle; C: Stretch-P_1 and D: variation of Stress-P_1 during one cardiac cycle).

around those neovessels that had undergone a large deformation, shown in Fig. 4. Further analysis indicated that there was no significant difference ($p = 0.087$) in terms of Stress-P_1 at systole between the groups without (without-RBC) and with (with-RBC) red blood cells (Table 1); however, during one cardiac cycle, with-RBC underwent greater Stress-P_1 variation (Diff-Stress-P_1) than without-RBC ($p < 0.0001$). The deformation of neovessels in with-RBC group at systole was about 8.9% which was much greater than the one in the without-RBC group (3.4%; $p < 0.0001$). During one cardiac cycle, the stretch variation (Diff-Stretch-P_1) of with-RBC was about 2.82%, while the value of without-RBC was only 0.87% ($p < 0.0001$). Furthermore, the lumen contour deformed (Diff-Area) much less in the without-RBC group than that in the with-RBC group (0.565% vs. 2.024%; $p < 0.0001$).

4. Discussion

To our knowledge, this is the first study to quantify the mechanical conditions around neovessels within atherosclerosis (Fig. 2). We highlight possible associations between intraplaque hemorrhage and these mechanical conditions (Fig. 4 and Table 1). We found first, that mechanical stress and stretch decreased significantly as the distance between the neovessel and the main arterial lumen increased (Fig. 3). Second, those neovessels with surrounding red blood cells, presumably evidence of fresh hemorrhage, underwent much larger deformation at systole and stress and stretch variations during one cardiac cycle than those without red blood cells close by (Table 1).

Several studies have shown a pathological effect of vessel stretch on the cellular and genetic environment of the plaque. The large cycle deformation may impede endothelial cell survival and tubulogenesis through the NAD(P)H subunit p22phox pathway [25]. Pathological stretch can dysregulate cytoskeletal gene expression, such as filamin A [26], affecting cell attachment and encouraging programmed cell death [27] and therefore preventing healing in the carotid plaque following acute events [28]. On a tissue level, the risk of elevated strain/deformation on plaque destabilization has been also recognized by various computational

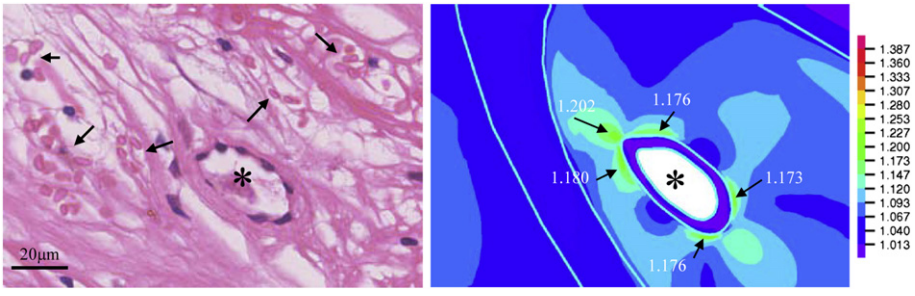

Fig. 4. Representative histology slide depicting a neovessel surrounded by red blood cells and the corresponding large local Stretch-P_1 during systole.

Table 1
Comparison of local maximum principal stress (Stress-P_1) and stretch (Stretch-P_1) and their variations (Diff-Stress-P_1 and Diff-Stretch-P_1) and change of lumen area (Diff-Area) during one cardiac cycle between neovessels with and without red blood cells (RBC) surrounded (the results were presented in Median [inter quartile range]).

	Stress-P_1 (kPa)	Diff-Stress-P_1 (kPa)	Stretch-P_1	Diff-Stretch-P_1	Diff-Area (%)
Without-RBC ($n = 233$)	12.8 [7.5, 25.1]	3.1 [1.6, 5.5]	1.034 [1.020, 1.067]	0.0087 [0.0045, 0.0185]	0.565 [0.220, 1.049]
With-RBC ($n = 146$)	16.3 [10.3, 27.1]	5.3 [3.4, 8.3]	1.089 [1.056, 1.131]	0.0282 [0.0190, 0.0427]	2.024 [1.208, 3.763]
p-Value	0.087	<0.0001	<0.0001	<0.0001	<0.0001

and clinical studies [28–30]. Although there are likely several biological processes at work in the promotion of intraplaque hemorrhage, here we suggest a possible contribution from the mechanical conditions around the neovessel.

The association between alterations in mechanical stress and plaque hemorrhage was suspected by Lusby et al. in early 1980s [31]. Recently, intraplaque hemorrhage has been recognized as one trigger of plaque vulnerability [32]. Monitoring the development of neovascularization within plaque might be important clinically. Non-invasive imaging techniques [33] such as contrast-enhanced magnetic resonance imaging (MRI) [34] and microbubble-targeted ultrasound [35], have been developed to quantify it. *In vivo* high-resolution elastography approaches, such as intravascular ultrasound [36], optical coherence tomography [37] and B-mode ultrasound elastography [38], have shown the capacity in quantifying the local tissues deformation in the atherosclerotic plaque. Further development of these techniques could lead to a more accurate plaque vulnerability assessment by integrating plaque compositional features and critical mechanical conditions.

Despite the interesting findings reported in our paper, some limitations exist: (1) the small number of plaques analysed ($n = 4$) means the pathological conclusions, such as the distribution pattern of neovessels and extravasated red blood cells ought to be repeated. However, this limitation does not completely negate our conclusion that large deformations around the neovessel might promote hemorrhage, because those four plaques yielded approximately 400 neovessels for analysis; (2) the origin of neovessel could be various. It may be from the vasa vasorum in the adventitia or due to the thrombus healing [39]. They are not differentiated in this study; another consideration is that (3) this study was a two-dimensional simulation, and the effect of the blood flow was not taken into account in this model. Since the neovessels were located within the plaque structure, high velocity blood flow in the main arterial lumen should have minimal impact on the prediction of critical mechanical conditions around the neovessel; lastly, (4) despite rigorous attention to detail, some distortion of the plaque samples may have occurred during processing for histopathological examination. Our segmentation, therefore might not represent the true *in vivo* configuration of the plaque.

In conclusion, we suggest that there are large degrees of deformation and high variation in the mechanical loading around plaque neovessels during the cardiac cycle. These factors might damage the vessel walls and, in conjunction with inflammatory and other factors, promote intraplaque hemorrhage.

Conflict of interest

None.

Acknowledgements

This research is supported by ARTreat European Union FP7, BHF PG/11/74/29100 and the NIHR Cambridge Biomedical Research Centre. Ms. He was supported by Cambridge-CSC (China Scholarship Council) International Scholarship. The authors thank Anita Shelley from the Department of Physiology, Development and Neuroscience, University of Cambridge, in acquiring the histopathological images.

References

[1] The global burden of disease: 2004 update. World Health Organization (WHO) Press; 2008.
[2] http://www.nhlbi.nih.gov/health/health-topics/topics/catd/ [Online].
[3] Inzitari D, Eliasziw M, Gates P, et al, North American Symptomatic Carotid Endarterectomy Trial Collaborators. The causes and risk of stroke in patients with asymptomatic internal-carotid-artery stenosis. New England Journal of Medicine 2000;342:1693–700.
[4] Golledge J, Greenhalgh RM, Davies AH. The symptomatic carotid plaque. Stroke 2000;31:774–81.
[5] Sadat U, Weerakkody RA, Bowden DJ, et al. Utility of high resolution MR imaging to assess carotid plaque morphology: a comparison of acute symptomatic, recently symptomatic and asymptomatic patients with carotid artery disease. Atherosclerosis 2009;207:434–9.
[6] Ota H, Yu W, Underhill HR, et al. Hemorrhage and large lipid-rich necrotic cores are independently associated with thin or ruptured fibrous caps: an in vivo 3T MRI study. Arteriosclerosis, Thrombosis, and Vascular Biology 2009; 29:1696–701.
[7] Eliasziw M, Streifler JY, Fox AJ, Hachinski VC, Ferguson GG, Barnett HJ. Significance of plaque ulceration in symptomatic patients with high-grade carotid stenosis. North American Symptomatic Carotid Endarterectomy Trial. Stroke 1994;25:304–8.
[8] Yuan C, Zhang SX, Polissar NL, et al. Identification of fibrous cap rupture with magnetic resonance imaging is highly associated with recent transient ischemic attack or stroke. Circulation 2002;105:181–5.
[9] Takaya N, Yuan C, Chu B, et al. Presence of intraplaque hemorrhage stimulates progression of carotid atherosclerotic plaques: a high-resolution magnetic resonance imaging study. Circulation 2005;111:2768–75.
[10] Altaf N, MacSweeney ST, Gladman J, Auer DP. Carotid intraplaque hemorrhage predicts recurrent symptoms in patients with high-grade carotid stenosis. Stroke 2007;38:1633–5.
[11] Altaf N, Daniels L, Morgan PS, et al. Detection of intraplaque hemorrhage by magnetic resonance imaging in symptomatic patients with mild to moderate carotid stenosis predicts recurrent neurological events. Journal of Vascular Surgery 2008;47:337–42.
[12] Sadat U, Teng Z, Young VE, et al. Association between biomechanical structural stresses of atherosclerotic carotid plaques and subsequent ischaemic cerebrovascular events – a longitudinal in vivo magnetic resonance imaging-based finite element study. European Journal of Vascular and Endovascular Surgery 2010;40:485–91.
[13] Takaya N, Yuan C, Chu B, et al. Association between carotid plaque characteristics and subsequent ischemic cerebrovascular events: a prospective assessment with MRI – initial results. Stroke 2006;37:818–23.
[14] Singh N, Moody AR, Gladstone DJ, et al. Moderate carotid artery stenosis: MR imaging-depicted intraplaque hemorrhage predicts risk of cerebrovascular ischemic events in asymptomatic men. Radiology 2009;252:502–8.
[15] Moreno PR, Purushothaman KR, Sirol M, Levy AP, Fuster V. Neovascularization in human atherosclerosis. Circulation 2006;113:2245–52.
[16] Milei J, Parodi JC, Alonso GF, Barone A, Grana D, Matturri L. Carotid rupture and intraplaque hemorrhage: immunophenotype and role of cells involved. American Heart Journal 1998;136:1096–105.
[17] Williams JK, Armstrong ML, Heistad DD. Vasa vasorum in atherosclerotic coronary arteries: responses to vasoactive stimuli and regression of atherosclerosis. Circulation Research 1988;62:515–23.
[18] Galili O, Sattler KJ, Herrmann J, et al. Experimental hypercholesterolemia differentially affects adventitial vasa vasorum and vessel structure of the left internal thoracic and coronary arteries. The Journal of Thoracic and Cardiovascular Surgery 2005;129:767–72.
[19] Virmani R, Kolodgie FD, Burke AP, et al. Atherosclerotic plaque progression and vulnerability to rupture: angiogenesis as a source of intraplaque hemorrhage. Arteriosclerosis, Thrombosis, and Vascular Biology 2005;25: 2054–61.
[20] Leclercq A, Houard X, Philippe M, et al. Involvement of intraplaque hemorrhage in atherothrombosis evolution via neutrophil protease enrichment. Journal of Leukocite Biology 2007;82:1420–9.
[21] Ribatti D, Levi-Schaffer F, Kovanen PT. Inflammatory angiogenesis in atherogenesis – a double-edged sword. Annals of Medicine 2008;40:606–21.

[22] Richardson PD, Davies MJ, Born GV. Influence of plaque configuration and stress distribution on fissuring of coronary atherosclerotic plaques. Lancet 1989;2:941–4.
[23] Tang D, Teng Z, Canton G, et al. Sites of rupture in human atherosclerotic carotid plaques are associated with high structural stresses: an in vivo MRI-based 3D fluid-structure interaction study. Stroke 2009;40:3258–63.
[24] Sadat U, Teng Z, Young VE, et al. Impact of plaque haemorrhage and its age on structural stresses in atherosclerotic plaques of patients with carotid artery disease: an MR imaging-based finite element simulation study. International Journal of Cardiovascular Imaging 2011;27:397–402.
[25] Kou B, Zhang J, Singer DR. Effects of cyclic strain on endothelial cell apoptosis and tubulogenesis are dependent on ROS production via NAD(P)H subunit p22phox. Microvascular Research 2009;77:125–33.
[26] D'Addario M, Arora PD, Ellen RP, McCulloch CA. Interaction of p38 and Sp1 in a mechanical force-induced, beta 1 integrin-mediated transcriptional circuit that regulates the actin-binding protein filamin-A. The Journal of Biological Chemistry 2002;277:47,541–47,550.
[27] Kainulainen T, Pender A, D'Addario M, Feng Y, Lekic P, McCulloch CA. Cell death and mechanoprotection by filamin a in connective tissues after challenge by applied tensile forces. The Journal of Biological Chemistry 2002;277:21,998–2,009.
[28] Teng Z, Sadat U, Huang Y, et al. In vivo MRI-based 3D mechanical stress-strain profiles of carotid plaques with juxtaluminal plaque haemorrhage: an exploratory study for the mechanism of subsequent cerebrovascular events. European Journal of Vascular and Endovascular Surgery 2011;42:427–33.
[29] Lee RT, Schoen FJ, Loree HM, Lark MW, Libby P. Circumferential stress and matrix metalloproteinase 1 in human coronary atherosclerosis. Implications for plaque rupture. Arteriosclerosis, Thrombosis, and Vascular Biology 1996;16:1070–3.
[30] Sadat U, Teng Z, Young VE, Graves MJ, Gaunt ME, Gillard JH. High-resolution magnetic resonance imaging-based biomechanical stress analysis of carotid atheroma: a comparison of single transient ischaemic attack, recurrent transient ischaemic attacks, non-disabling stroke and asymptomatic patient groups. European Journal of Vascular and Endovascular Surgery 2011;41:83–90.
[31] Lusby RJ, Woodcock JP, Machleder HI, et al. Transient ischaemic attacks: the static and dynamic morphology of the carotid artery bifurcation. British Journal of Surgery 1982;69(Suppl.):S41–4.
[32] Michel JB, Virmani R, Arbustini E, Pasterkamp G. Intraplaque haemorrhages as the trigger of plaque vulnerability. European Heart Journal 2011;32:1977–85. 1985a, 1985b, 1985c.
[33] Purushothaman KR, Sanz J, Zias E, Fuster V, Moreno PR. Atherosclerosis neovascularization and imaging. Current Molecular Medicine 2006;6:549–56.
[34] Cornily JC, Hyafil F, Calcagno C, et al. Evaluation of neovessels in atherosclerotic plaques of rabbits using an albumin-binding intravascular contrast agent and MRI. Journal of Magnetic Resonance Imaging 2008;27:1406–11.
[35] Leong-Poi H, Christiansen J, Klibanov AL, Kaul S, Lindner JR. Noninvasive assessment of angiogenesis by ultrasound and microbubbles targeted to alpha(v)-integrins. Circulation 2003;107:455–60.
[36] Baldewsing RA, Schaar JA, de Korte CL, Mastik F, Serruys PW, van der Steen AF. Intravascular ultrasound elastography: a clinician's tool for assessing vulnerability and material composition of plaques. Studies in Health Technology and Informatics 2005;113:75–96.
[37] Rogowska J, Patel NA, Fujimoto JG, Brezinski ME. Optical coherence tomographic elastography technique for measuring deformation and strain of atherosclerotic tissues. Heart 2004;90:556–62.
[38] Dumont DM, Doherty JR, Trahey GE. Noninvasive assessment of wall-shear rate and vascular elasticity using combined ARFI/SWEI/spectral Doppler imaging system. Ultrasonic Imaging 2011;33:165–88.
[39] Geremia G, Brack T, Brennecke L, Haklin M, Falter R. Occlusion of experimentally created fusiform aneurysms with porous metallic stents. AJNR American Journal of Neuroradiology 2000;21:739–45.